Prabha Materials Science Letters
Vol. 3, No. 1, 46-59, 2024
https://doi.org/10.33889/PMSL.2024.3.1.003

Ram Arti Publishers

Estimation of Dimensional Deviation of Parts Printed in Different Orientations on Multi Jet Printer

Ramesh Chand
Department of Industrial and Production Engineering,
Dr. B. R. Ambedkar National Institute of Technology, Jalandhar, Punjab, India.
Corresponding author: rameshchandjanjua@gmail.com

M. K. Gupta
Department of Mechanical Engineering,
Opole University of Technology, Opole, Poland.
E-mail: munishguptanit@gmail.com

(Received on October 25, 2023; Revised on November 17, 2023; Accepted on November 25, 2023)

Abstract
The study was primarily concerned with the dimensional deviation for the part produced in the various alignments A, B, C, & D and selecting the orientation or alignments through the least dimensional deviation. In this work, the part is lying on the base (A), the long edge (B), and the short edge (C), and the part is inclined at 45 degrees (D) to the surface of the base plate. Created the components in a variety of orientations using a multi-jet printer. Further, using experimental data (change in length, width, height and diameter), the model has been developed with a regression-based imperial connection to predict the behavior of MultiJet-three-dimensional (MJP-3D) printed components in various orientations. Because the goal was to anticipate the optimum orientation, the Graph Theory and Matrix Approach Method (GTMA) were utilized towards discover the best orientation. In contrast to other orientations, orientation C is determined to be the optimum manufacturing orientation with the least dimensional variation.

Keywords- AM, Orientation, MCDM, Multi Jet three-dimensional, Dimensional accuracy.

1. Introduction

Recently, Additive Manufacturing (AM) has become the quickest and fastest production technology among many manufacturing activities (Aktürk et al., 2021; Mo et al., 2022; Singh, 2023). It can produce components with fewer waste, a smaller amount of material (polymer), less weight and at a reduced price (Gupta et al., 2023). In the automobile industry, AM methods have been referred to as the "fourth industrial revolution." Compared to conventional production, this is due to its layer-by-layer adding method, resulting in the removal of sophisticated fixtures, cutting tools, highly skilled labor, lighter, cleaner, and shorter lead time (Özdemir and Korkmaz, 2023). Thus, additive manufacturing contributes to improving the functioning and efficiency of mechanical components, particularly those used in automobiles (Korkmaz et al., 2022).

Several kinds of AM methods have been developed thus far. ASTM F2792 categorized it into seven distinct types. One of these types of MJP is the additive manufacturing process used in Material Jetting. Through the jetting nozzles, it deposits the liquid material and the support material in the right form and fill pattern, layer by layer. After all layers are complete, the final product may be built with little scrap and maximum durability. The manufactured parts required post-processing in a heated oil bath (52-65°C) to separate the support material (wax) from the primary material (polymer). Each AM process has many process parameters that change according on the method, technology, hardware/components used, environment, material, and so on. The goal of optimization is to predict the best-optimized parameters

based on the requirements, which may vary depending on applications, quantity, and cost. Table 1 outlines the parameters available for several AM procedures. Geometric accuracy, microstructure, fractures, hardness, porosity, residual stress, surface roughness, mechanical properties, thermal properties, dilution, crystallographic orientations, processing time, and cost are only some of the other aspects that are affected by building orientation. Material-jetting-based AM components manufactured in different orientations are limited in surface polish, strength, accuracy, and printing time. As a result, component orientation optimization must be performed to utilize any standard techniques such as graph theory and matrix approach methodology. This research aims to establish the most efficient material jetting orientation for producing a finished product. There are four different MJP component orientations that must be adhered to in accordance with the MJP machine standard. To this end, we use Graph Theory and Matrix Approach (GTMA) methods, as a part of Multiple Criterion Decision-Making (MCDM) techniques. The impact of various component orientations on dimensional deviation is assessed using GTMA technique as a result of the part's application in the automobile industry.

Table 1. Process parameters across several AM methods.

AM Process	Process Parameters	References
Additive manufacturing via extrusion	There are a number of factors that may affect the quality of a print job, including infill, raster width, raster angle, build, Layer thickness orientation, nozzle temperature, nozzle feed rate, density, infill pattern, contour width, and print speed.	Chadha et al. (2019), Zaman et al. (2019).
Metal additive manufacturing	Factors such as laser strength, build platform distance, beam current, scan rate, hatch volume, probe size on powder, part orientation, and scan path must all be taken into account. Scanning rate, layer thickness, and pattern are all factors to consider about.	Zaman et al. (2019).
Sheet lamination	Factors to think about include layer thickness, heater temperature, platform retracts, heater speed, laser speed, feeder speed, and platform speed.	Mekonnen et al. (2016).
Material jetting	Construction orientation, post-curing duration, layer thickness, and material all have an influence.	Yap et al. (2017).
Binder jetting	Considerations include the spread speed, powder level, drying time, sintering, binder material, and printing saturation.	Shrestha and Manogharan (2017).
VAT polymerization	Hatch spacing, layer thickness, post-curing period, and orientation are some of the most crucial factors.	Chockalingam et al. (2006), Zhou et al. (2000).
Powder bed fusion	Power of the laser, speed of the scan, distance of the hatch, temperature of the bed, thickness of the layer, size of the spot, beam profile, temperature of the working environment, interval time, and scanning mode	Arısoy et al. (2017).

2. Background Work on Additive Manufacturing

From last 30 years, AM technology has been used in more and more applications. Based on fuzzy Analytical Hierarchy Process (AHP) - Technique For Order Of Preference By Similarity To Ideal Solution (TOPSIS), Anand and Vinodh rank AM processes and determine the optimal parameters. (Anand and Vinodh, 2018). Sheoran and Kumar (2020) aims to summarize recent studies of statistical and experimental design methods (e.g., Taguchi, GA, grey relational, RSM, fractional factorial, ANN, Fuzzy logic, ANOVA, etc.) for a variety of applications or output responses (e.g., enhancing mechanical properties, reducing build time, improving part quality, etc.) (Sheoran and Kumar, 2020). Ghaleb et al implemented process selection using Vlse Kriterijumska Optimizacija I Kompromisno Resenje (VIKOR), AHP, and TOPSIS. The authors reported that the VIKOR and TOPSIS methods were better suited to choosing manufacturing processes due to their flexibility throughout the decision-making process, quantity of available processes and criteria, suitability in supporting a group option, and ability to add or remove a criterion (Ghaleb et al., 2020). Papakostas et al used the developing, deploying, and using an agent-based decision support platform. The authors claim that the suggested method might also supplement current platforms and approaches by, for example, giving information on the cost and time performance of various process configurations so that only a small number of configurations are

examined in these platforms (Papakostas et al., 2020). Singh et al. (2015) provides a technique based on graph theory and the matrix method for determining the suitability of titanium for ultrasonic machining. Using graph theory and the matrix approach, a mathematical function has been developed to identify different machining characteristics and their relative importance. The results show that an experimental run using a tool material of titanium, a grit size of 500, and a power supply of 300 W produces optimum machinability outcomes (Singh et al., 2015). Huang et al. (2021) presents a Fuzzy Power Weighted Maclaurin Symmetric Mean (FPWMSM) operator based on Hamacher T-norm and T-conorm (HTT), as well as a generic approach based on this operator for tackling MCDM issues in AM design. The provided technique comprises primarily of fuzzification, normalization, and aggregate of criteria values and the creation of alternative sequences. The findings indicate that the technique is practical and successful in capturing the interplay of criterion and risk attitude. decision-makers and lessen the impact of extremes criterion values on decision-making outcomes (Huang et al., 2021). Dobrovolskienė and Pozniak (2021) provides an actual application and comparison of two distinct MCDM methods to evaluate the sustainability of a real estate project. The study's findings indicated a substantial disparity in the rankings produced by SAW and TOPSIS. Furthermore, the TOPSIS technique is more sensitive to changes in baseline data than the SAW method, according to the findings of the MCDM sensitivity study (Dobrovolskienė & Pozniak, 2021). Bogojević et al. (2020) studied on the influence of AM orientation on the fatigue behaviour of steel parts. The parts were made from Maraging Steel EOS MS1 and stainless steel EOS PH_1 using direct laser metal sintering technique. Three different sets of samples were made for each material, with the long axis tilted at 0, 45, and 90 degrees with respect to the horizontal construction plane. According to the findings, the fatigue strength of maraging steel samples is unaffected by the orientation of the structure. However, as compared to horizontal or vertical axis orientation, the fatigue strength of angled stainless steel samples is up to 20% higher (Bogojević et al., 2020).

Among many research investigations, there is a gap in applying the empirical relationship by which one may estimate the dimensional deviation of the fabricated component in different orientations. The literature study utilized many MCDM techniques to determine the optimal manufacturing orientation for different AM techniques. However, the Graph Theory & Matrix Approach (GTMA) is less employed. So, in this article, GTMA identifies the optimum orientation with the least amount of dimensional variation among four different orientations.

3. Materials and Procedures

3.1 Dimensional Analysis

Precision and repeatability are also significant advantages of 3D printing for producing complicated forms and geometries. As a result, the accuracy and repeatability of the MJP-based 3D printer are being studied in this study. Accuracy and repair ability are evaluated by using many configurations of the same component. Using the space that is available on the base plate effectively is the reason for the various configurations of the same components. If the entire area of the base plate is not used for comparable parts, it will raise the cost of each unit. However, the dimensional variation will be insufficient to fulfill industrial requirements. To investigate the different geometries and the dimensional accuracy of the MJP-fabricated components. The planned portion is a mix of a rectangle, cylinder, and fillets. These shapes allow users to investigate the linear and radial dimensions of the product in various orientations. The product is aligned with faces 2, 4, 1, and inclined 45^o with faces 1 and 2 in orientations A, B, C, and D.VisiJet M2R-WT (the material designation supplied by 3D systems) is used for all of the parts (Chand et al., 2023).

In this work, MJP 3D printer has been used to create the 3D component. The printer's technical specifications include printing mode (HD), net build volume (XYZ) 294 x 211 x 144 mm, resolution

(XYZ) 800 x 900 x 790 DPI (Dots Per Inch), and 32 (micron) layers. VisiJet-M2 -SUP is the sole entirely cured support material for Project MJP2500, and it is compatible with all of the printer's materials. After manufacturing the item on the MJP 3D printer, the produced part is post-processed. During the post-processing, the component is immersed in an oil bath warmed to 50-60°C for 10 minutes (Chand et al., 2023). The measurements were performed with CMM machine.

4. Estimation of Dimensional Deviation using Regression Model

There are sixteen linear equations developed for various orientations (A, B, C, D) and four parameters (height, length, width, and diameter). After the range for which the linear regression model equations are valid, these equations may forecast the behavior of each parameter. The dimensional deviation in orientation A is shown in Figure 1.

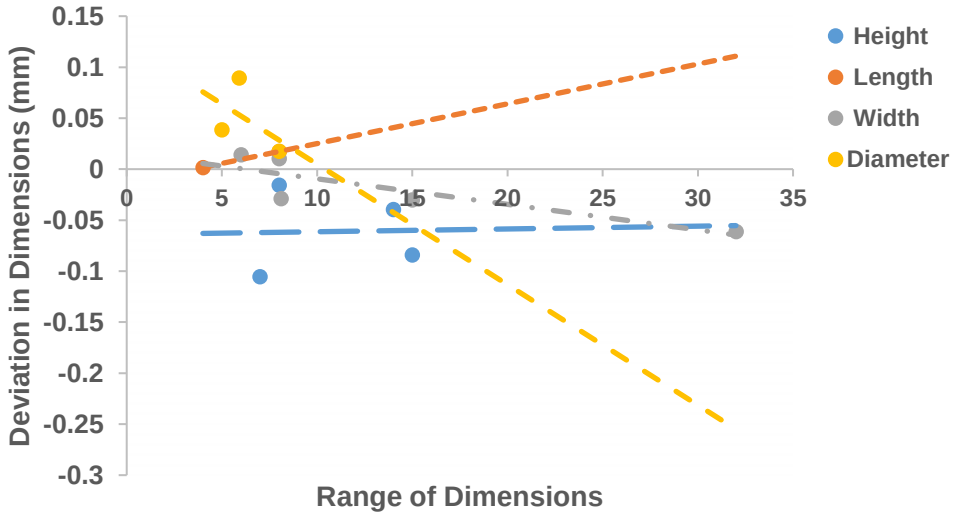

Figure 1. Dimensional deviation in orientation A.

In orientation A, the base plate makes contact with the portion throughout its whole surface area. Consider Equation (1) as a Deviation in length (DIL) trend line valid within a range of 4-8 mm. It was discovered in equation one that when the component's size grew more than 8 mm in the X-Y plane along the X-axis, the final part would be +0.1 mm. Equation (2), which is valid for the Deviation in width (DIW) in the X-Y plane along the y-axis, within the range of 6-32 mm, reflects that up to 32 mm dimensional deviation is -0.05 mm. Equation (3) is valid for the Deviation in height (DIH) within the range of 7-15 mm. The plane normal to the X-Y plane reflects that dimensional deviation is negligibly small. Equation (4) is valid for the analysis of Deviation in diameter (DID in the range of 5-8 mm, reflecting that, the diameter of the hole will be oversized by +0.1 mm within the range of 0.5-0.08 mm. If the diameter of the hole is more than 15-32 mm. The diameter of the hole will be undersized within the range of -0.1 to -0.25 mm.

$$\mathrm{DIL} = 0.0039 \times \mathrm{L} - 0.0138 \quad (\text{range } 4 - 8 \text{ mm}) \tag{1}$$

$$DIW = -0.0025 \times \mathrm{W} + 0.0156 \quad (\text{range } 6 - 32 \text{ mm}) \tag{2}$$

$$DIH = 0.0003 \times H - 0.0641 \quad (\text{range } 7 - 15 \text{ mm}) \tag{3}$$

$$DID = -0.0118 \times D + 0.123 \quad (\text{range } 5 - 8 \text{ mm}) \tag{4}$$

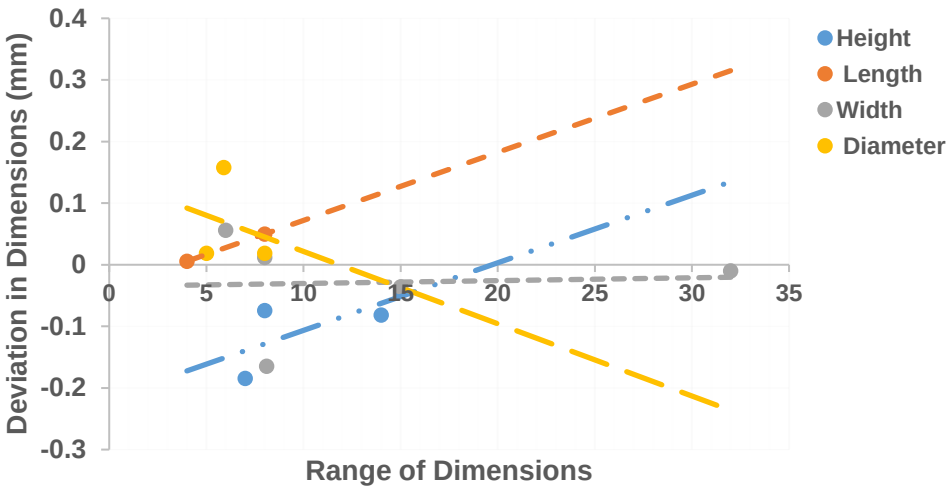

Figure 2. Dimensional deviation in orientation B.

Orientation B reduces the part's contact area with the base plate. To forecast the dimensional variation for the length, using trend line Equation (5) within the range of 4-8 mm. Beyond 8 mm in length, the slope of the line in terms of dimensional deviation continues to rise. After 8 mm to 32 mm, a +0.3 mm dimensional difference is allowed. Equation (6) forecasts the dimensional variation for a width range of 6-32 mm. Dimensional divergence is decreasing. Equation (7) is effective for forecasting height behavior in the Z-axis between 7 and 15 mm. Parts were discovered to be undersized -0.1 mm in the height range of 7-15 mm. After 15 mm, the part gets bigger by +0.1 mm increments up to 32 mm. Equation (8) is valid for diameters ranging from 5-8 mm. For the diameter range, the 5-15 mm hole was oversized by +0.1 mm, from 16 mm to 32 mm, the diameter of the hole was undersized by -0.2 mm. The dimensional deviation in Orientation B is shown in Figure 2.

$$\mathrm{DIL} = 0.0111 \times \mathrm{L} - 0.0385 \quad (5)$$

$$DIW = 0.0005 \times W - 0.035 \quad (6)$$

$$DIH = 0.011 \times H - 0.2162 \quad (7)$$

$$DID = -0.0117 \times D + 0.139 \quad (8)$$

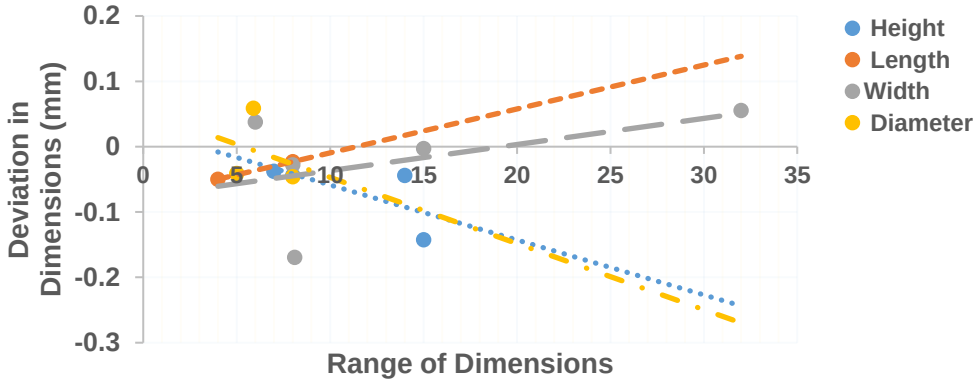

Figure 3. Dimensional deviation in orientation C.

The part is angled at 90° to the base plate for orientation C. The component's surface area in contact with the base plate is less in orientation C compared to A and B. Equation (9) is quite valuable and applicable in the 4-8 mm range. According to equation 9, when the length range increases over 8 mm, the slope of the line increases. As the part's length approaches 32 mm, it will become +0.15 mm oversized. Equation (10) is important to predict the behavior of dimensional deviation for width. Equation (10) is correct over a range of 6-32 mm. it may predict the dimensional deviation behavior of width after the stated range. It has been discovered that up to 32 mm, the manufactured part will be +0.05 mm oversized. Equation (11) is valid for heights ranging from 7 to 15 mm. The components will be undersized by -0.025 mm for a dimensional range from 8 mm to 32 mm. For diameters range from 5-8 mm, Equation (12) is valid. The hole was undersized by -0.25 mm up to 32 mm after the stated diameter limit. The dimensional deviation in Orientation C is shown in Figure 3.

$$DIL = 0.0067 \times L - 0.0767 \quad (9)$$

$$DIW = 0.004 \times W - 0.0766 \quad (10)$$

$$DIH = -0.0084 \times H + 0.0255 \quad (11)$$

$$DID = -0.0101 \times D + 0.0543 \quad (12)$$

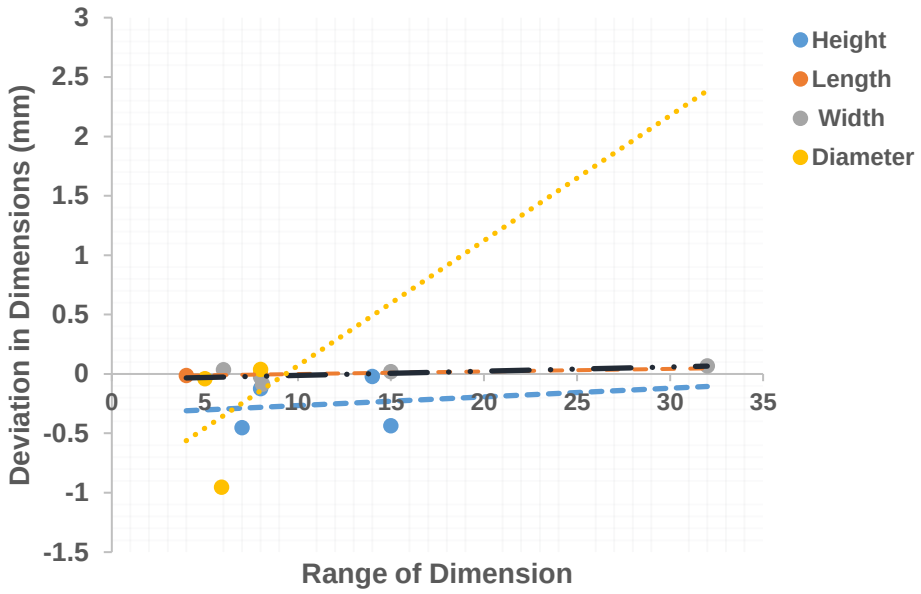

Figure 4. Dimensional deviation in orientation D.

The portion is slanted at 45° to the base plate for orientation D. Equation (13) is applicable for lengths ranging from 4 to 8 mm. Beyond the specified range, dimensional variation up to 32 mm does not represent any dimensional deviation. In terms of width, Equation (14) is correct over the range 6-32 mm and does not indicate any dimensional discrepancy. The height range of 7-15 mm is covered by Equation (15). In predicting the dimensional deviation exceeding 15 mm, it is discovered that the dimensional deviation is decreasing. Equation (16) is valid for diameters ranging from 7 to 15 mm. The manufactured holes were undersized by -0.05 mm between 7 to 10 mm. The diameter of the hole was anticipated to be +2 mm large after 10 to 32 mm. The dimensional deviation in Orientation D is shown in Figure 4.

$$DIL = 0.0022 \times L - 0.0222 \quad (13)$$

$$DIW = 0.0035 \times W - 0.0474 \quad (14)$$

$$DIH = 0.0073 \times H - 0.3391 \quad (15)$$
$$DID = 0.1053 \times D - 0.9829 \quad (16)$$

a. Finding the Best Regression Model Basics Orientation

Dimensions ranging from 7 to 32 mm are utilized in the manufactured part. The only common criterion utilized to select the optimal orientation among the four orientations is 8 mm. The discovered Orientations C and D were to be the optimal orientations when the dimensional variation is less than 0.02 mm. These obtained equations will be advantageous in predicting the behavior of the parameters (height, length, width, and diameter) when the parameter range is expanded beyond the range utilized in the current study. The dimensional deviation in different orientations is shown in Figure 5.

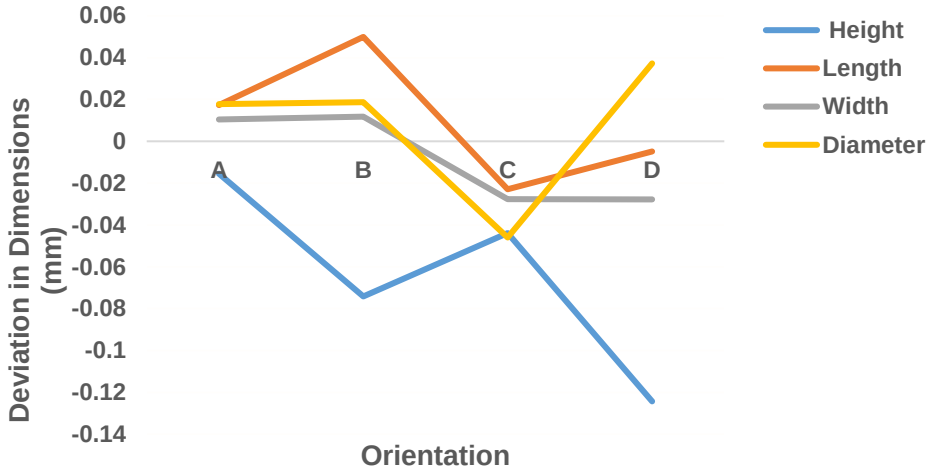

Figure 5. Dimensional deviation in different orientations.

5. The Optimal Orientation is Determined Using a Matrix-Based Technique and Graph Theory

One of the approaches accessible is Graph Theory & Matrix-Based Approach (GTMA), which can provide insight into the challenge of picking the appropriate orientation, as this technique combines the relative significance, it also uses digraph to graphically express the characteristics and their interdependence (Rao et al., 2019). This approach is well-organized and rational, and it has been verified and confirmed in a variety of scientific and technological domains (Chand et al., 2023).This paper suggested a graph theory and matrix-based methodology evaluate the optimal orientation among four orientations during MJP-based 3D printing. The dimensional attribute digraph and matrix approach analyze and quantify many attributes that impact the Dimensional Deviation (DD). A Permanent Dimensional Deviational Index (PDDI) is used to determine the ideal orientation. GTMA technique is a systematic and logical idea that is beneficial for evaluating and modeling many applications in engineering and many other fields (Chand et al., 2023). The digraph is used to graphically illustrate the qualities and their relative relevance in terms of DD. The matrix then converts the attribute digraph into a mathematical representation. The PDDI is calculated using mathematical representation, i.e., a constant function. As a result, the purpose of this paper is to introduce GTMA for determining the appropriate orientation in MJP-based 3D printing. The primary stages for executing the strategy mentioned above are outlined below.

a. Selection of Attributes

In this first step, we identify a variety of parameters that affect the Dimensional Accuracy (DA) of an MJP-based 3D printed part. The experimental design that satisfies the DA of the fabricated part is finalized. Using Table 2 and Table 3 from (Chand et al., 2023), we can determine the attribute values (T_i) and weights (u_{ij}).

b. Dimensional Deviation Attributes Digraph Representation

The components that have an effect on DA and their connections to one another are shown as vertices and edges in a digraph. A digraph is a graph with two sets of nodes, each labelled Q=T_i, and two sets of directed edges, R=u_{ij}, where i=1, 2,..., X. Each edge represents the relative importance of the nodes, and each node T_i represents the i^{th} dimensional characteristic. The DD procedure examines the same number of Dimensional Deviation Attributes (DDA) regardless of the number of nodes (X) that are traversed. Four important characteristics are selected for the analysis of DD in all four directions: (1) Deviation of Length (DOL), (2) Deviation of Width (DOW), (3) Deviation of Height (DOH), and (4) Deviation of Diameter (DOD). Figure 6 shows the digraph representation of the dimensional deviation attribute used in this study.

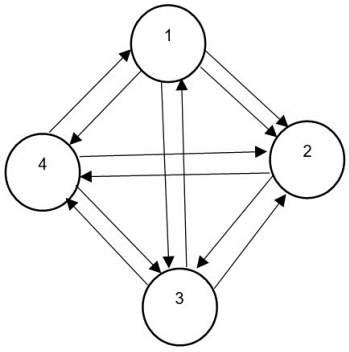

Figure 6. The dimensional deviation characteristics digraph for the MJP-based 3D printed part: ((1) Dimensional length deviation. (ii) Dimensional width deviation. (iii) Dimensional height deviation. (iv) Dimensional diameter deviation).

c. A Scalar Representation of the Digraph of the Properties of Dimensional Deviation

Dimensional deviation evaluation matrices (H) or the Variable Permanent Matrix for Permanent Dimensional Deviation index (PDDI) are necessary forms in which the digraph may be represented. All of the attributes (like T_i) and their weights (u_{ij}) are taken into account in the X*X matrix. The matrix given by Equation (17) is represented by the DD evaluation digraph. The diagonal parts T_1, T_2, T_3, and T_4 represent the inheritance of these four basic traits, while the off-diagonal components of the matrix illustrate the interdependence of these qualities (Rao and Gandhi, 2002).

The matrix H for the considered DD characteristics digraph is shown as: (PDDI) = H,

$$H = \begin{array}{c} Attributes \\ 1 \\ 2 \\ 3 \\ \cdots \\ \cdots \\ X \end{array} \begin{bmatrix} 1 & 2 & 3 & 4 & \ldots & \ldots & X \\ T_1 & u_{12} & u_{13} & u_{14} & \ldots & .. & u_{1X} \\ u_{21} & T_2 & u_{23} & u_{24} & \ldots & \ldots & u_{2X} \\ u_{31} & u_{32} & T_3 & u_{34} & \ldots & \ldots & u_{4X} \\ \ldots & \ldots & \ldots & \ldots & \ldots & \ldots & \ldots \\ \ldots & \ldots & \ldots & \ldots & \ldots & \ldots & \ldots \\ u_{X1} & u_{X2} & u_{X3} & u_{X4} & \ldots & \ldots & T_X \end{bmatrix} \quad (17)$$

The following is a representation of this PDDI for the DD attributes digraph under consideration.

$$H=\begin{array}{c} Attributes \\ \text{DOL} \\ \text{DOW} \\ \text{DOH} \\ \text{DOD} \end{array}\begin{bmatrix} \text{DOL} & \text{DOW} & \text{DOH} & \text{DOD} \\ T_1 & u_{ij} & u_{ik} & u_{il} \\ u_{ji} & T_2 & u_{jk} & u_{jl} \\ u_{ki} & u_{kj} & T_3 & u_{kl} \\ u_{li} & u_{lj} & u_{lk} & T_4 \end{bmatrix} \quad (18)$$

Variable Permanent function representation.

This matrix H, denoted as per (H), defines the permanent dimensional deviation function (PDDF). DD evaluation represents the DD qualities of the different orientations A, B, C, and D that were studied for this work. Furthermore, because there is no negative sign in the statement, this strategy prevents any loss of information (Rao et al., 2019).

The PDDI' is expressed in sigma form as:

$$\text{Per} \quad (H)=\prod_{i=1}^{X} T_i + \sum_{i,j,\ldots X}(u_{ij}u_{ji})T_kT_i \ldots\ldots\ldots T_X + \sum_{i,j..X}(u_{ij}u_{jk}u_{ki} + u_{ik}u_{kj}u_{ji})T_1T_m \ldots . T_X + \{\sum_{i,j\ldots.X}(u_{ij}u_{ji})(u_{kl}u_{lk})T_mT_n \ldots\ldots T_X + \sum_{i,j\ldots.X}(u_{ij}u_{jk}u_{kl}u_{li})(u_{il}u_{lk}u_{kj}u_{ji})T_mT_n \ldots\ldots . . T_X\} + [\sum_{i,j\ldots.X}(u_{lm}u_{ml})(u_{ij}u_{jk}u_{ki} + u_{ik}u_{kj}u_{ji})T_nT_o \ldots\ldots T_X + \sum_{i,j\ldots X}(u_{ij}u_{jk}u_{kl}u_{lm}u_{mi} + u_{im}u_{ml}u_{lk}u_{kj}u_{ji})T_nT_o \ldots\ldots . . T_X] + [(\sum_{i,j\ldots X}(u_{mn}u_{nm})(u_{ij}u_{jk}u_{kl}u_{li} + u_{il}u_{lk}u_{kj}u_{ji})T_o \ldots . T_X + \sum_{i,j\ldots.X}(u_{ij}u_{jk}u_{ki} + u_{ik}u_{kj}u_{ji})(u_{lm}u_{mn}u_{nl} + u_{ln}u_{nm}u_{ml})T_0 \ldots T_X + \sum_{i,j\ldots X}(u_{ij}u_{ji})(u_{kl}u_{lk})(u_{mn}u_{nm})T_0 \ldots\ldots T_k + \sum_{i,j..X}(u_{ij}u_{jk}u_{kl}u_{lm}u_{mn}u_{ni} + u_{in}u_{nm}u_{ml}u_{lk}u_{kj}u_{ji})T_0 \ldots . . T_X)] \ldots . \quad (19)$$

d. Permanent Dimensional Deviation Index (PDDI) Evaluation

For calculating the PDDI, the PDDF stated in Equation (19) is used. The term PDDI refers to the numerical value of the PDDF.

It is recommended that all numerical T_i values be normalized to the same scale (from 0 to 10) that is used for qualitative values. When assigning values of 0 and 10 to positive DD characteristics, smaller range values (T_{is}) and larger range values (T_{ib}), respectively, apply. Equation (20) suggests that intermediate values for T_{ii} might also be assigned on a scale from 0 to 10 for the qualities.

$T_i = (10/T_{ib})*T_{ii}$ for $T_{is} = 0$ (20)

$T_i = ((10/(T_{ib}-T_{is}))*(T_{ii}-T_{is})$ for $T_{is}>0$.

Table 2. Quantification of factors affecting dimensional deviation of 3D printed part.

Qualitative measure of factors affecting Dimensional deviation of 3D printed part	Assigned value of machinability factors (T_i)
Exceptionally low	0
Extremely low	1
Very low	2
Below average	3
Average	4
Above average	5
Moderate	6
High	7
Very high	8
Extremely high	9
Exceptionally high	10

A number of 0 indicates a wider range (T_{is}) and a value of 10 indicates a narrower range (T_{ib}) for negative DD traits. It is possible to assign intermediate values T_{ii} of the attributes on a scale from 0 to 10 as shown in Equation (21).

$$T_i = 10\ (1- (T_{ii} /T_{ib})) \quad \text{for } T_{is} =0 \tag{21}$$

$$T_i =((10/(T_{ib}-T_{is}))*(T_{ib}-T_{ii}) \text{ for } T_{is}>0.$$

Relative interdependence between two characteristics (i.e., u_{ij}) for a particular DD is likewise assigned a value between 0 and 10 and is classified into six groups. The degree of interdependence between two qualities may be measured on a scale of 0 to 10, as shown below:

$$u_{ij}= 10-u_{ji} \tag{22}$$

Table 3. Relative importance of dimensional deviation attributes (u_{ij}).

Category Description	Interdependencies of Attributes	
	u_{ij}	$u_{ji}=10-u_{ij}$
Two attributes are of equal importance	5	5
One attribute is slightly more important than the other	6	4
One attribute is more important than the other	7	3
One attribute is much more important than the other	8	2
One attribute is extremely more important than the other	9	1
One attribute is exceptionally more important than the other	10	0

The orientation with the highest possible PDDI value is selected as the optimal one.

6. Application of The Method for Determining the Best Orientation for a MJP-Based 3d Printed Part

The graph theory and matrix technique were used to determine the optimal orientation for a 3D printed MJP part (Rao and Padmanabhan, 2007).The results of the experiments are shown in Table 4 as the difference between the measured value and the actual value for the component made in the different orientations.

Table 4. Experimental results of Dimensional deviation in MJP based 3D printed part.

Orientations	Deviation of Height	Deviation of Length	Deviation of Width	Deviation of Diameter
A	-0.01547	0.01732	0.01042	0.0177
B	-0.07413	0.0499	0.01177	0.01872
C	-0.04392	-0.02293	-0.02771	-0.04598
D	-0.1243	-0.00493	-0.02779	0.03721

Graph theory and the matrix method consist of the following procedures:

a. Attribute Selection and Normalization of Experimental Findings

Used the following methods for deciding on DD features and for standardizing the many trial outcomes:

The DD attributes are recognized, and the characteristics evaluated are the deviations of height (DOH), length (DOL), width (DOW), and diameter (DOD). All of the characteristics mentioned above are regarded as non-beneficial. Table 5 displays the results of vector sum normalisation, Equations (20) and (21), applied to the values of various DD features for the various experimental runs. The interaction of features (i.e. u_{ij}) is likewise given numerical values between 0 and 10 in accordance with Table 6 and Equation (22) (Rao and Padmanabhan, 2006). u_{ij} is assigned 0.5 for all the attributes because all the attributes are non-beneficial attributes. Figure 7 depicts a permanent DDA digraph that comprises the DD attributes under consideration and their interrelationships.

Table 5. Dimensional deviation attribute values (T_i) for the problem considered.

Orientations	DOH	DOL	DOW	DOD
A	1.101754	0.70031	1.031855	0.725655
B	1.487592	0.136574	1.030505	0.709845
C	1.288885	1.396761	1.069985	1.712678
D	1.817586	1.085304	1.070065	0.423255

Table 6. Relative importance of dimensional deviation attributes (u_{ij}).

Attributes	DOH	DOL	DOW	DOD
DOH	…….	0.5	0.5	0.5
DOL	0.5	…….	0.5	0.5
DOW	0.5	0.5	…….	0.5
DOD	0.5	0.5	0.5	……..

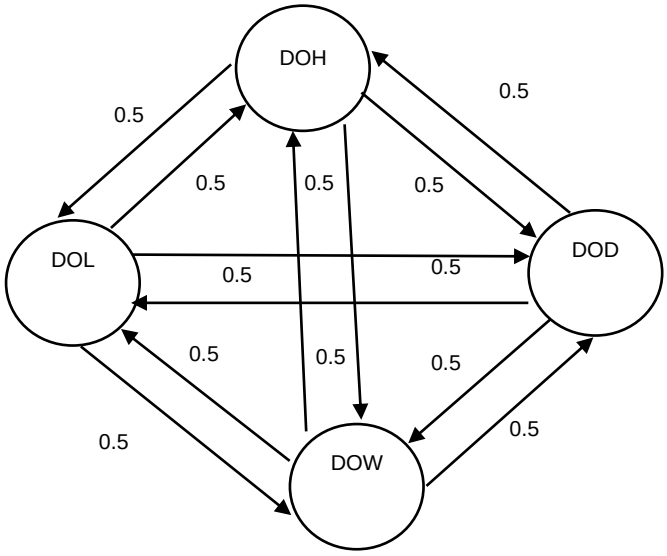

Figure 7. The relative relevance of the four properties of dimensional deviation (1. DOH, 2. DOL, 3. DOW, and 4. DOD) is shown in a digraph.

b. The Characteristics Matrix of Permanent Dimensional Deviation and the Variable Permanent Dimensional Deviation Function are Represented as Matrices (PDDF)

The equation represents the PDDA matrix H for the examined MJP-based 3D printer case (refer Equation 23).

$$H=\begin{matrix} Attributes \\ DOL \\ DOW \\ DOH \\ DOD \end{matrix}\begin{bmatrix} DOL & DOW & DOH & DOD \\ T_1 & u_{ij} & u_{ik} & u_{il} \\ u_{ji} & T_2 & u_{jk} & u_{jl} \\ u_{ki} & u_{kj} & T_3 & u_{kl} \\ u_{li} & u_{lj} & u_{lk} & T_4 \end{bmatrix} \quad (23)$$

The PDDF for the above matrix H, Equation (23), is

$$Per(H)=\prod_1^3 T_i + \sum_{i,j,k}(u_{ij}u_{ji})T_k + \sum_{i,j,k}(u_{ij}u_{jk}u_{ki} + u_{ik}u_{kj}u_{ji}) \quad (24)$$

c. The Numerical Value of the Permanent Dimension Deviation Index (PDDI) is Computed

The value of the PDDI is determined using the data from Tables 2 and 3. This index is calculated using the T_i and u_{ij} values from each experimental run. Table 7 shows the PDDI values for the various orientations in descending order.

Table 7. Values of permanent dimensional deviation index in descending order.

Orientation	Permanent Dimensional Deviation Index
C	8.00514
D	4.2451
A	3.20199
B	2.49256

According to the various values of the PDDI for different orientations, orientation C provides the best PDDI, followed by four other orientations.

7. Conclusions

The evaluation of the optimal 3D printing orientation for the MJP-based process is addressed in this study utilizing GTMA approach. This technique includes dimensional deviation attribute digraphs, attribute matrix representations, a permanent dimensional deviation function, various attributes index, which defines the accuracy of MJP based 3D printed parts in different orientations. The following findings may be derived from the study.

- Dimensional deviations can be estimated using empirical equations for different orientations.
- A GTMA method is proposed and validated as the optimal approach to the orientation of producing 3D printed components. Because of its flexibility, this method is better suited to solving a broad variety of issues encountered during 3D printing. The current study identifies numerous dimensional deviation parameters that determine the accuracy of an MJP-based 3D printed part. The results show that orientation C has the highest permanent dimensional deviation index value.
- The suggested strategy, based on graph theory and the matrix method, may be used to optimize a wide range of correlated responses of interest under the influence of different input parameters in any MJP (VisiJet M2R-WT) problem.

Conflict of Interest

No potential conflict of interest was reported by the author(s).

Acknowledgements

The whole work is financed by Dr. B. R. Ambedkar National Institute of Technology, Jalandhar, Punjab, India.

References

Aktürk, M., Boy, M., Gupta, M.K., Waqar, S., Krolczyk, G.M., & Korkmaz, M.E. (2021). Numerical and experimental investigations of built orientation dependent Johnson–Cook model for selective laser melting manufactured AlSi10Mg. *Journal of Materials Research and Technology*, *15*, 6244-6259.

Anand, M.B., & Vinodh, S. (2018). Application of fuzzy AHP–TOPSIS for ranking additive manufacturing processes for microfabrication. *Rapid Prototyping Journal*, *24*(2), 424-435. https://doi.org/10.1108/RPJ-10-2016-0160.

Arısoy, Y.M., Criales, L.E., Özel, T., Lane, B., Moylan, S., & Donmez, A. (2017). Influence of scan strategy and process parameters on microstructure and its optimization in additively manufactured nickel alloy 625 via laser powder bed fusion. *The International Journal of Advanced Manufacturing Technology*, *90*, 1393-1417. https://doi.org/10.1007/s00170-016-9429-z.

Bogojević, N., Ćirić-Kostić, S., Vranić, A., Olmi, G., Croccolo, D. (2020). Influence of the Orientation of Steel Parts Produced by DMLS on the Fatigue Behaviour. In: Wang, L., Majstorovic, V., Mourtzis, D., Carpanzano, E., Moroni, G., Galantucci, L. (eds) *Proceedings of 5th International Conference on the Industry 4.0 Model for Advanced Manufacturing*. Lecture Notes in Mechanical Engineering. Springer, Cham. https://doi.org/10.1007/978-3-030-46212-3_22.

Chadha, A., Ul Haq, M.I., Raina, A., Singh, R.R., Penumarti, N.B., & Bishnoi, M.S. (2019). Effect of fused deposition modelling process parameters on mechanical properties of 3D printed parts. *World Journal of Engineering*, *16*(4), 550-559.

Chand, R., Sharma, V.S., Trehan, R., Gupta, M.K., & Sarikaya, M. (2023). Investigating the dimensional accuracy and surface roughness for 3D printed parts using a multi-jet printer. *Journal of Materials Engineering and Performance*, *32*(3), 1145-1159. https://doi.org/10.1007/s11665-022-07153-0.

Chockalingam, K., Jawahar, N., Ramanathan, K.N., & Banerjee, P.S. (2006). Optimization of stereolithography process parameters for part strength using design of experiments. *The International Journal of Advanced Manufacturing Technology*, *29*, 79-88.

Dobrovolskienė, N., & Pozniak, A. (2021). Simple Additive Weighting versus Technique for Order Preference by Similarity to an Ideal Solution: which method is better suited for assessing the sustainability of a real estate project. *Entrepreneurship and Sustainability Issues*, *8*(4), 180-196.

Ghaleb, A.M., Kaid, H., Alsamhan, A., Mian, S.H., & Hidri, L. (2020). Assessment and comparison of various MCDM approaches in the selection of manufacturing process. *Advances in Materials Science and Engineering*, *2020*, 1-16. https://doi.org/10.1155/2020/4039253.

Gupta, M.K., Korkmaz, M.E., Shibi, C.S., Ross, N.S., Singh, G., Demirsöz, R., Jamil, M., & Królczyk, G.M. (2023). Tribological characteristics of additively manufactured 316 stainless steel against 100 cr6 alloy using deep learning. *Tribology International*, *188*, 108893.

Huang, M., Chen, L., Zhong, Y., & Qin, Y. (2021). A generic method for multi-criterion decision-making problems in design for additive manufacturing. *The International Journal of Advanced Manufacturing Technology*, *115*, 2083-2095. https://doi.org/10.1007/s00170-021-06832-x.

Sheoran, A.J., & Kumar, H. (2020). Fused deposition modeling process parameters optimization and effect on mechanical properties and part quality: Review and reflection on present research. *Materials Today: Proceedings*, *21*, 1659-1672. https://doi.org/10.1016/j.matpr.2019.11.296.

Korkmaz, M.E., Waqar, S., Garcia-Collado, A., Gupta, M.K., & Krolczyk, G.M. (2022). A technical overview of metallic parts in hybrid additive manufacturing industry. *Journal of Materials Research and Technology*, *18*, 384-395.

Mekonnen, B.G., Bright, G., & Walker, A. (2016). A study on state of the art technology of laminated object manufacturing (LOM). In *CAD/CAM, Robotics and Factories of the Future: Proceedings of the 28th International Conference on CARs & FoF 2016* (pp. 207-216). Springer, New Delhi, India.

Mo, F., Guo, B., Liu, Q., Ling, W., Liang, G., Chen, L., Yu, S., & Wei, J. (2022). Additive manufacturing for advanced rechargeable lithium batteries: A mini review. *Frontiers in Energy Research*, *10*, 986985.

Özdemir, M.T., & Korkmaz, M.E. (2023). A short and technical review on lattice structures produced by additive manufacturing. *Prabha Materials Science Letters*, *2(1)*, 48-61.

Papakostas, N., Newell, A., & George, A. (2020). An agent-based decision support platform for additive manufacturing applications. *Applied Sciences*, *10*(14), 4953. https://doi.org/10.3390/app10144953.

Rao, R.V., & Gandhi, O.P. (2002). Digraph and matrix methods for the machinability evaluation of work materials. *International Journal of Machine Tools and Manufacture*, *42*(3), 321-330.

Rao, R.V., & Padmanabhan, K.K. (2006). Selection, identification and comparison of industrial robots using digraph and matrix methods. *Robotics and Computer-Integrated Manufacturing*, *22*(4), 373-383.

Rao, R.V., & Padmanabhan, K.K. (2007). Rapid prototyping process selection using graph theory and matrix approach. *Journal of Materials Processing Technology*, *194*(1-3), 81-88.

Rao, R.V., Rai, D.P., & Balic, J. (2019). Multi-objective optimization of abrasive waterjet machining process using Jaya algorithm and PROMETHEE Method. *Journal of Intelligent Manufacturing*, *30*, 2101-2127.

Shrestha, S., & Manogharan, G. (2017). Optimization of binder jetting using Taguchi method. *JOM*, *69*, 491-497.

Singh, J.P. (2023). Materials towards the development of li rechargeable thin film battery. *Prabha Materials Science Letters*, *2*(1), 26-40. https://doi.org/10.33889/pmsl.2023.2.1.003.

Singh, R.P., Kumar, J., Kataria, R., & Singhal, S. (2015). Investigation of the machinability of commercially pure titanium in ultrasonic machining using graph theory and matrix method. *Journal of Engineering Research*, *3*, 35 https://doi.org/10.7603/s40632-015-0035-2.

Yap, Y.L., Wang, C., Sing, S.L., Dikshit, V., Yeong, W.Y., & Wei, J. (2017). Material jetting additive manufacturing: An experimental study using designed metrological benchmarks. *Precision Engineering*, *50*, 275-285.

Zaman, U.K.U., Boesch, E., Siadat, A., Rivette, M., & Baqai, A.A. (2019). Impact of fused deposition modeling (FDM) process parameters on strength of built parts using Taguchi's design of experiments. *The International Journal of Advanced Manufacturing Technology*, *101*, 1215-1226.

Zhou, J.G., Herscovici, D., & Chen, C.C. (2000). Parametric process optimization to improve the accuracy of rapid prototyped stereolithography parts. *International Journal of Machine Tools and Manufacture*, *40*(3), 363-379.